



## Supporting Information

for *Adv. Sci.*, DOI: 10.1002/adv.201902372

Fibroblast Growth Factor 2-Mediated Regulation of Neuronal Exosome Release Depends on VAMP3/Cellubrevin in Hippocampal Neurons

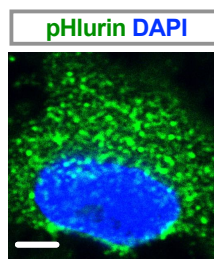
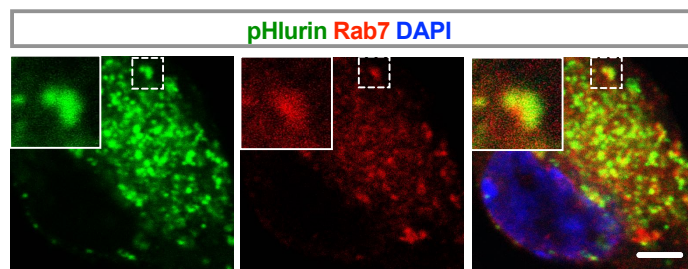
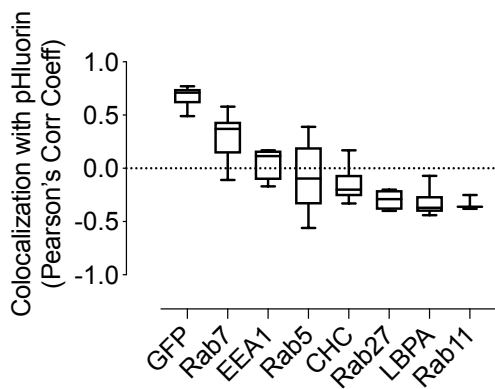
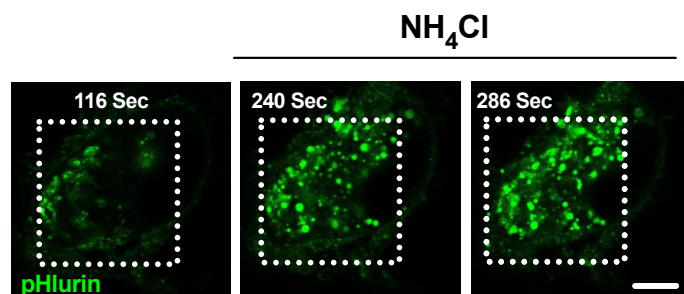
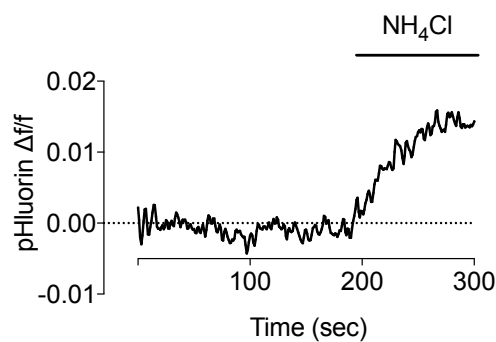
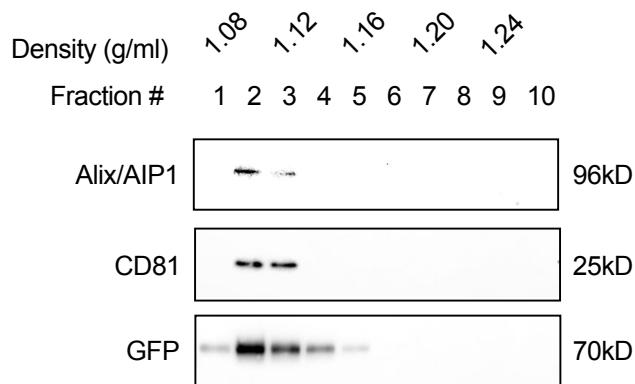
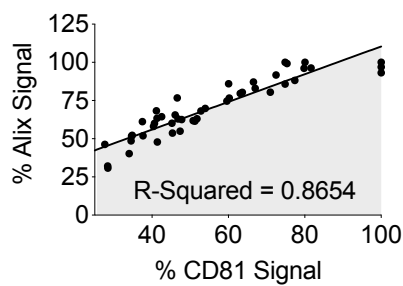
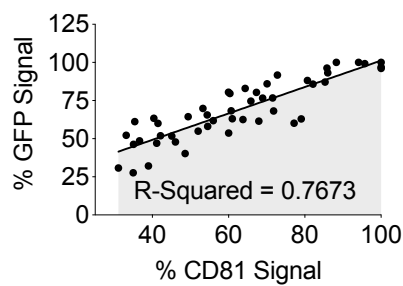
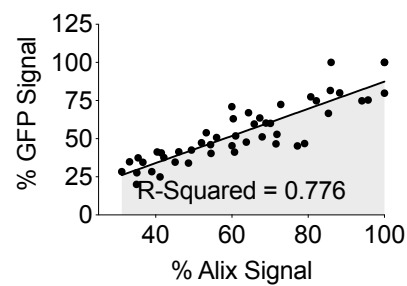
*Rohit Kumar, Qilin Tang, Stephan A. Müller, Pan Gao, Diana Mahlstedt, Sofia Zampagni, Yi Tan, Andreas Klingl, Kai Bötzel, Stefan F. Lichtenthaler, Günter U. Höglinger, and Thomas Koeglsperger\**

## **Supporting Information:**

### **Fibroblast Growth Factor 2-mediated Regulation of Neuronal Exosome Release Depends on VAMP3/cellubrevin in Hippocampal Neurons.**

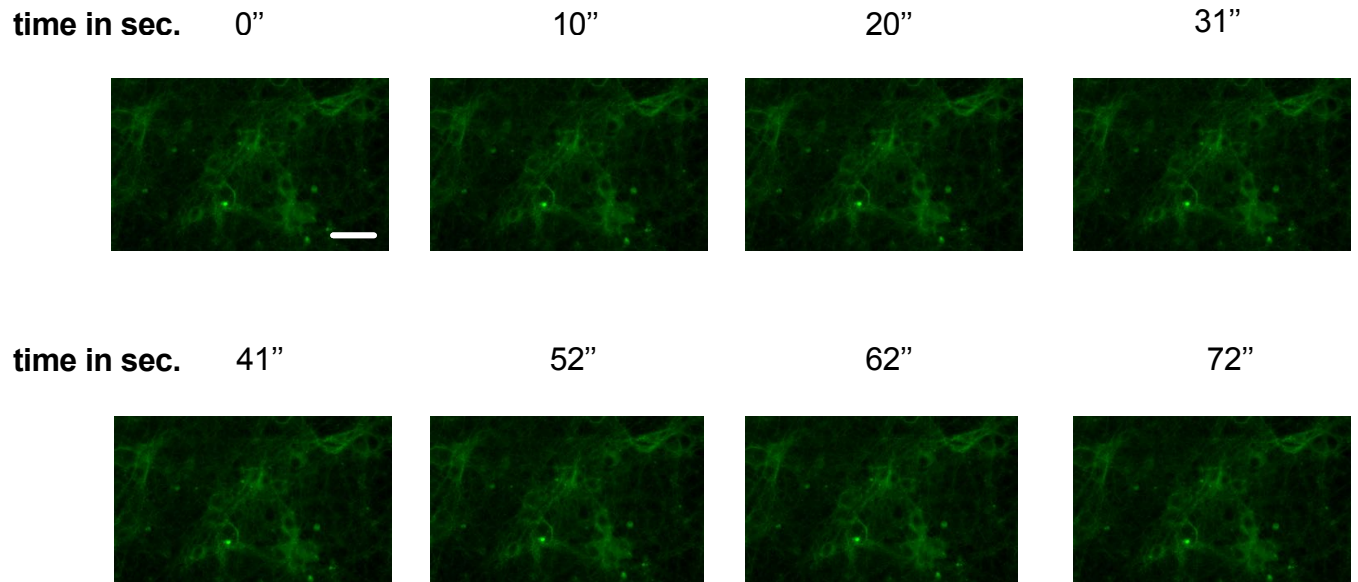
*Rohit Kumar, Qilin Tang, Stephan A. Müller, Pan Gao, Diana Mahlstedt, Sofia Zampagni, Yi Tan, Andreas Klingl, Kai Bötzel, Stefan F. Lichtenthaler, Günter Höglinger & Thomas Koeglsperger\**

# Figure S1

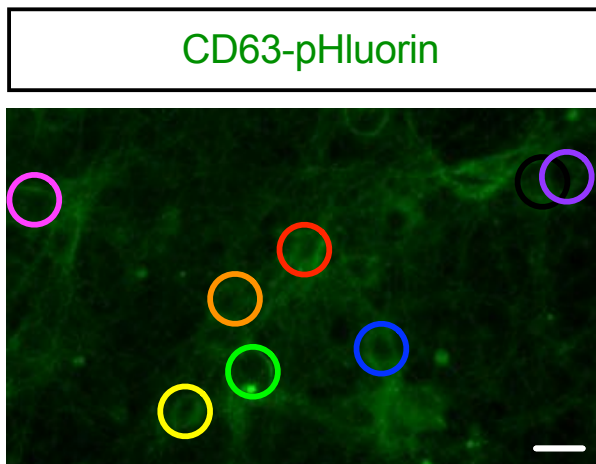
**a****b****c****d****e****f****g****h****i**

# Figure S2

**a**



**b**



**c**

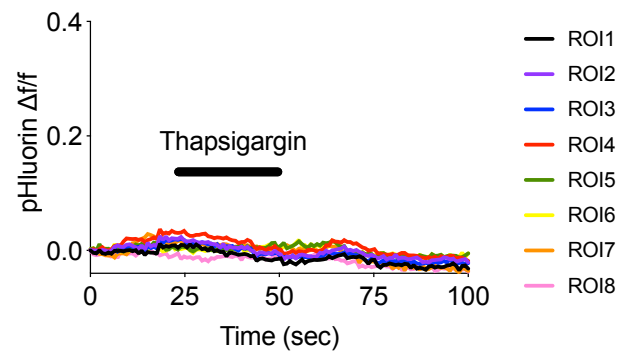
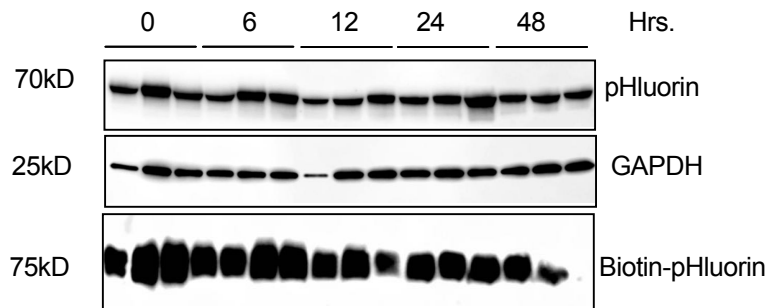
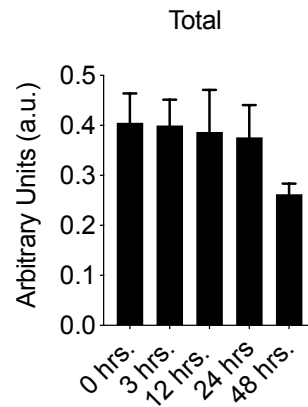


# Figure S3

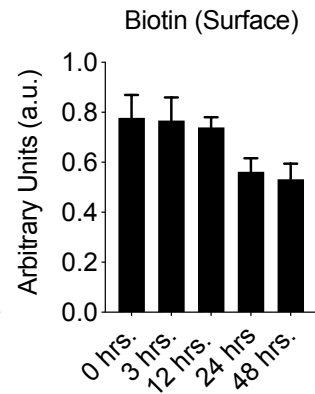
**a**



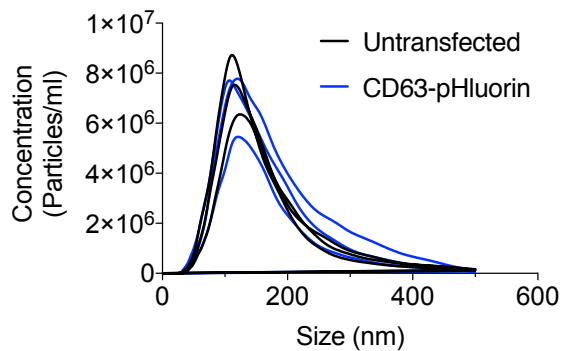
**b**



**c**



**d**



**e**

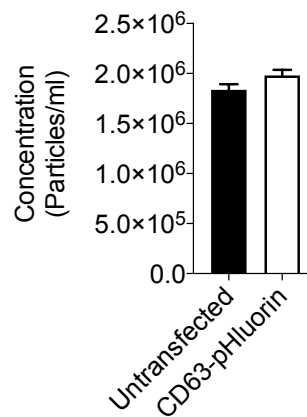
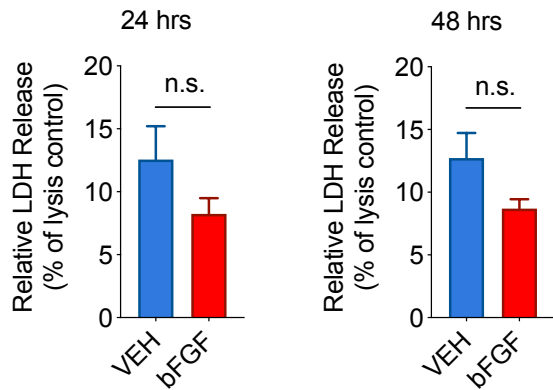
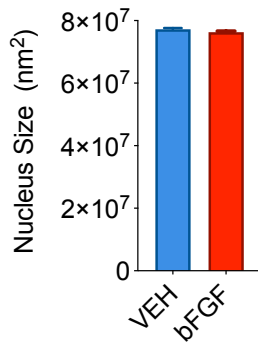


# Figure S4

**a**



**b**



**c**

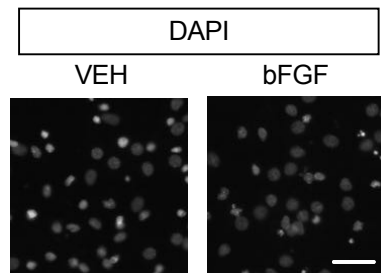


# Figure S5

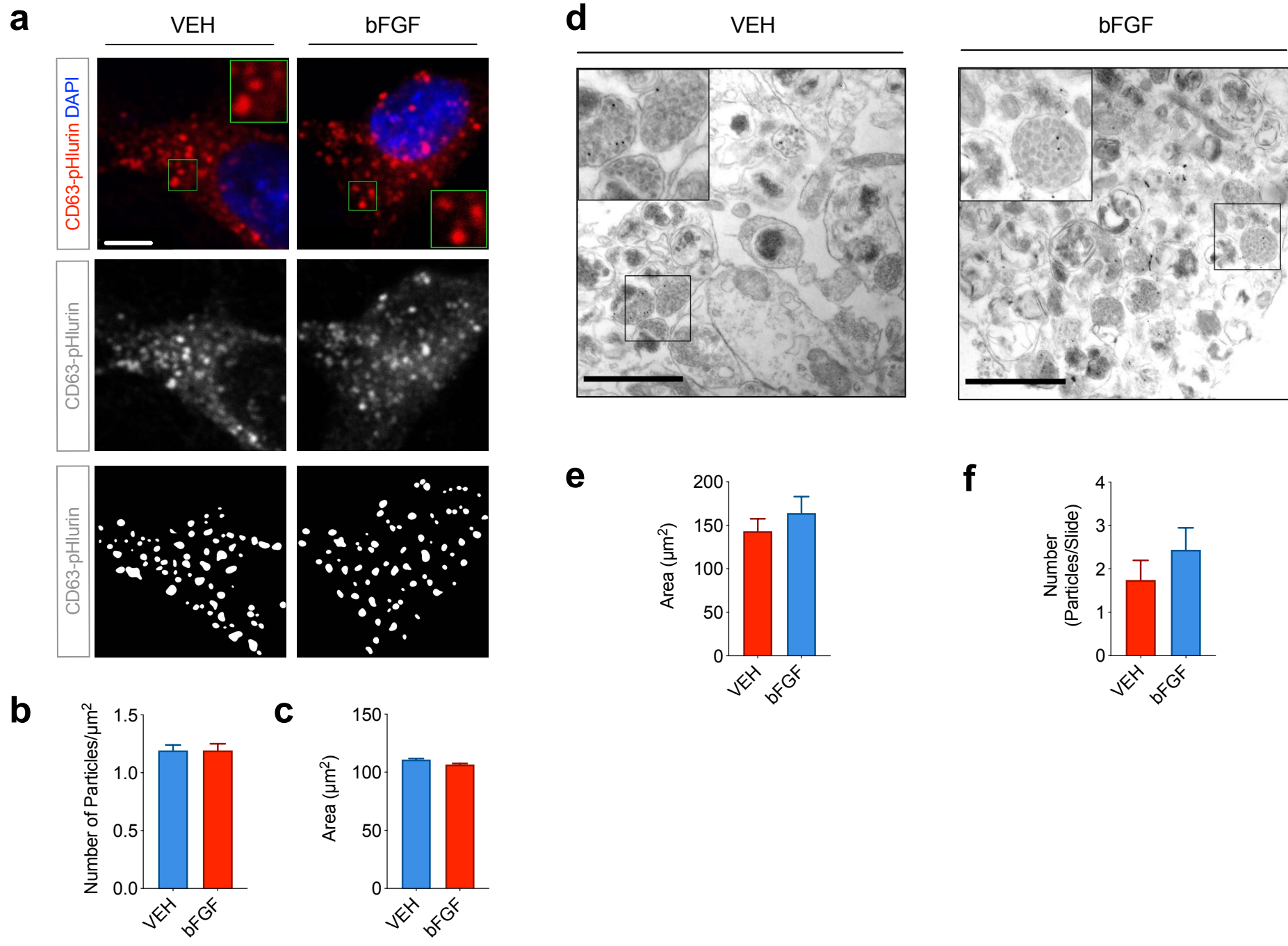


# Figure S6

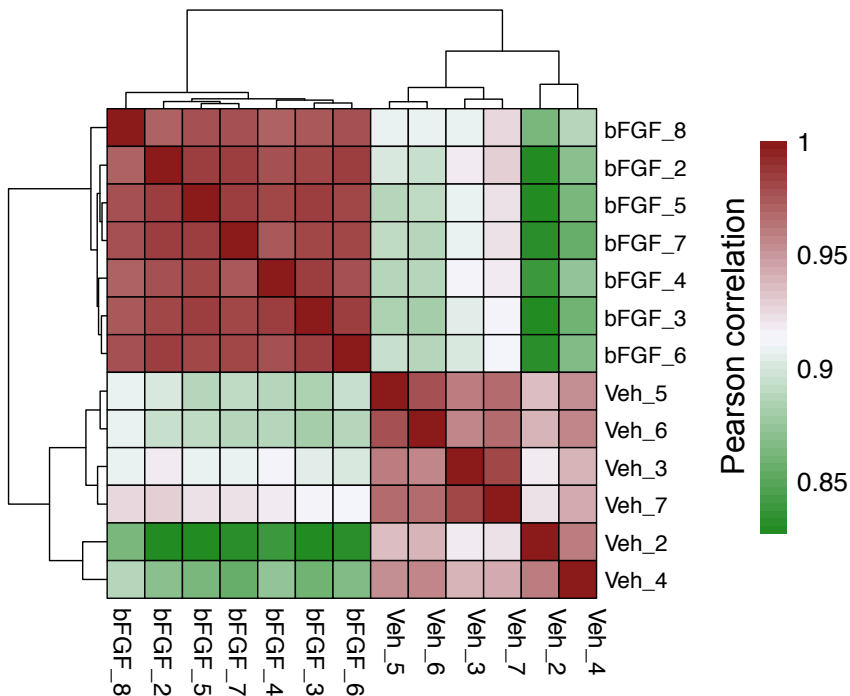
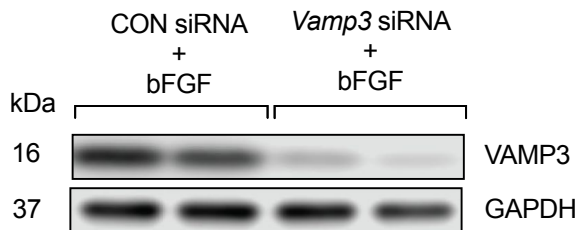


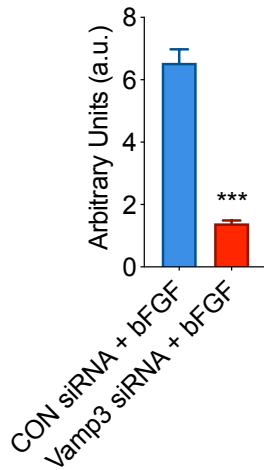


# Figure S7

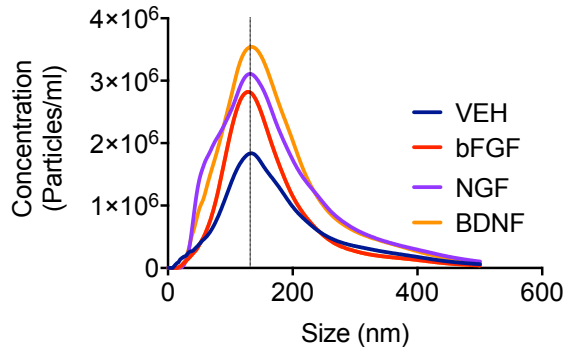
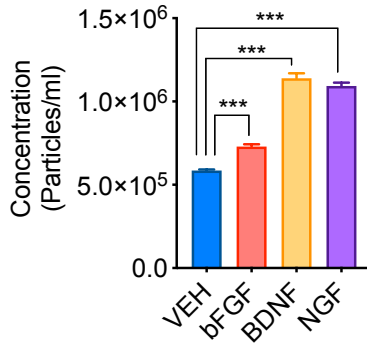
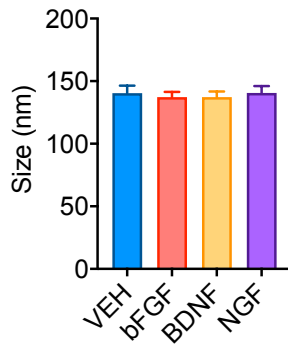
**a**



**b**

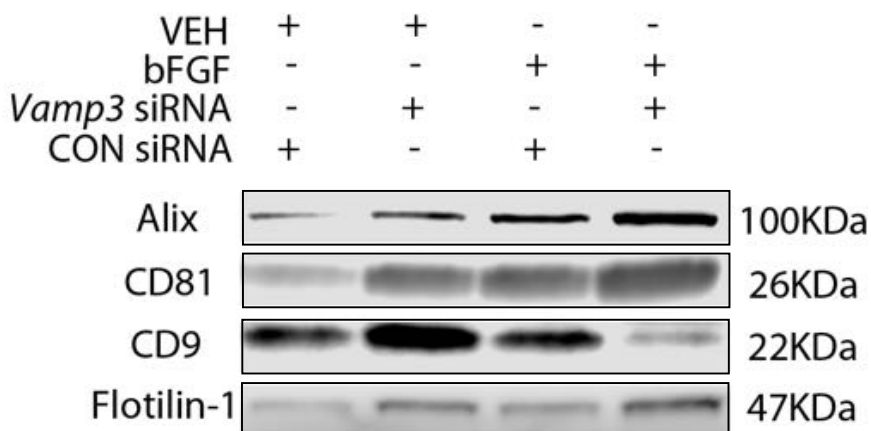


# Figure S8

**a****b****c**

# Figure S9

**a**



**b**

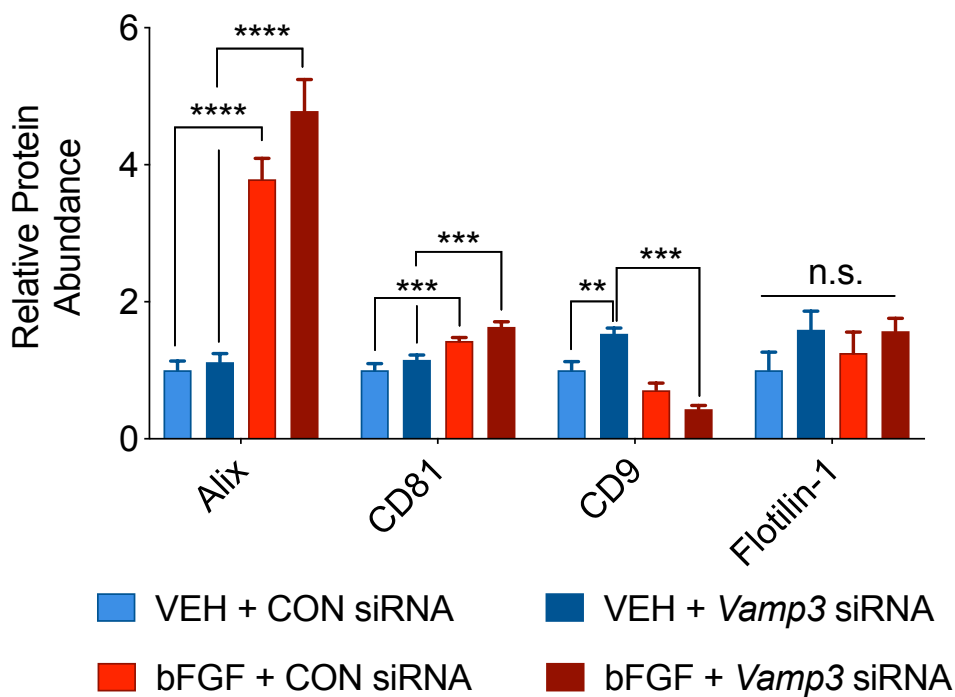
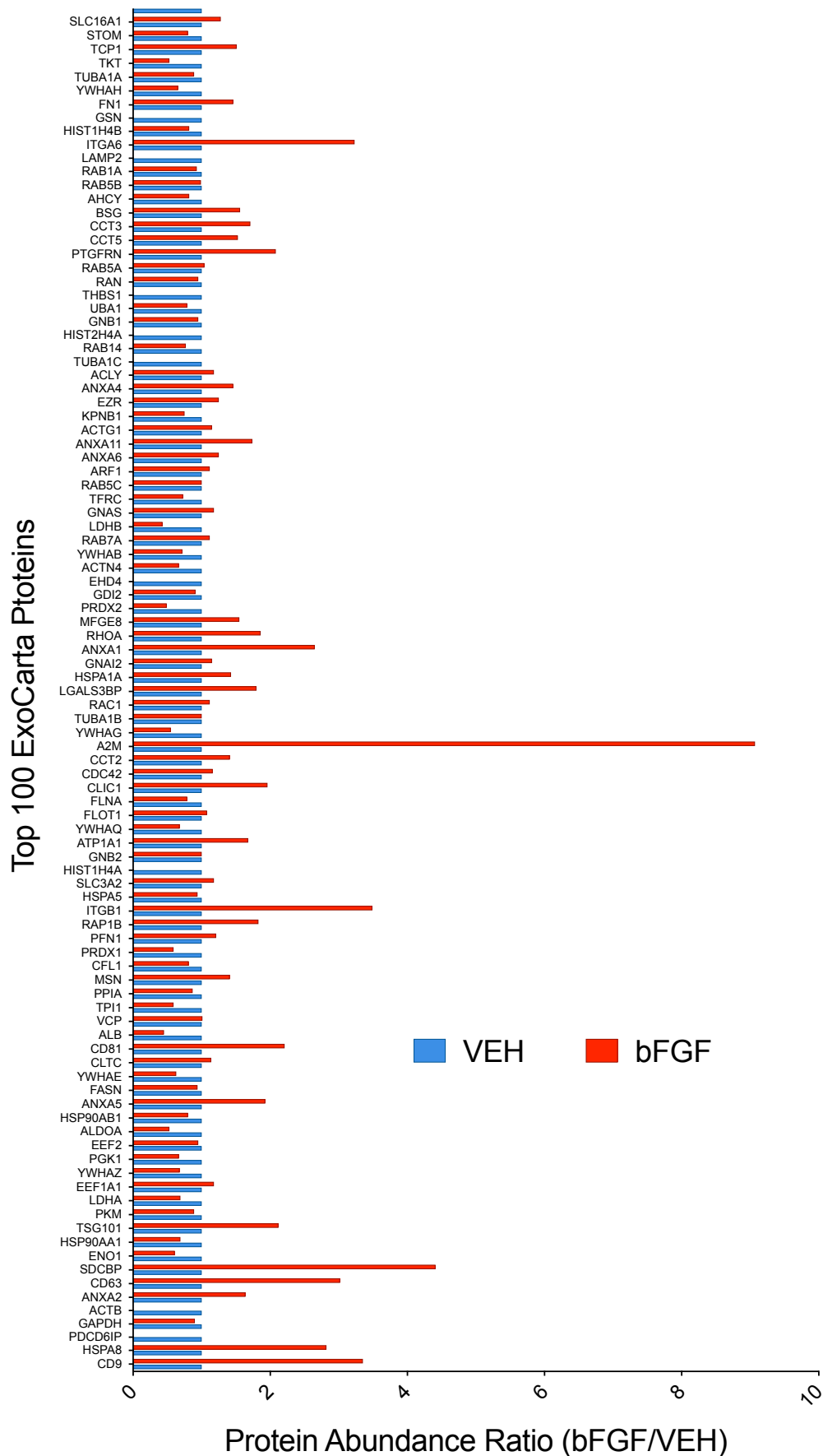


# Figure S10



**Supplementary Figure Legends:****Figure S1: CD63-pHluorin is tagged to extracellular vesicles (EVs) and co-localizes with Rab7-positive late endosomes in rat hippocampal neurons. a)**

Photomicrograph illustrating the lentiviral expression of *p*CD63-pHluorin in rat hippocampal neurons at day 10 post transduction (DPT). Scale bar: 3.5  $\mu$ m **b)**

Immunocytochemical staining (ICC) from CD63-pHluorin-transduced neurons stained with an antibody against Rab7 (red) and counterstained with DAPI (blue). Scale bar: 3.5  $\mu$ m. **c)** Bar graph showing the Pearson's correlation coefficient (PCC) for CD63-

pHluorin with different antigens of the endolysosomal pathway. As expected, the highest PCC was obtained from correlating the pHluorin signal with the signal from a

GFP antibody, followed by Rab7. **d)** Photomicrographs demonstrating an increase in GFP-fluorescence in response to perfusion of CD63-pHluorin-transfected neurons with

50 mM  $\text{NH}_4\text{Cl}$ . Scale bar: 5.5  $\mu$ m. **e)** Graph illustrating the  $\text{NH}_4\text{Cl}$ -evoked pHluorin fluorescence signal as a function of time. **f)** Western blot illustrating the segregation

of GFP, CD81 and Alix/AIP1 to different iodixanol densities. Alix/AIP1 and CD81 segregate to densities of 1.10 to 1.12, whereas GFP exhibited a broader distribution,

indicating the heterogeneity of GFP-positive extracellular vesicles (EVs). **g-i)** Graphs illustrating the correlation of the signal intensities between different EV markers in

each Western blot ( $n = 48/\text{antibody}$ ). For correlation, a linear regression has been conducted and an R-squared calculated.

**Figure S2 Thapsigargin has no immediate effect on neuronal EV release. a)**

Photomicrographs from cultured hippocampal neurons imaged during the application

of thapsigargin (1  $\mu$ M). Scale bar: 50  $\mu$ m. **b,c**) Application of thapsigargin (10  $\mu$ M) has no effect on pHluorin fluorescence. Coloured circles indicate the region of interest (ROIs) from which the signal was analysed and displayed over time. Scale bar: 25  $\mu$ m.

**Figure S3: Treatment with bFGF has no effect on the expression of CD63-pHluorin or on EV release.** **a**) Western blot illustrating the abundance of total pHluorin, biotinylated (= surface) pHluorin and GAPDH. **b,c**) Bar graphs illustrating the total and surface pHluorin in cultured hippocampal neurons treated with bFGF for 3, 12, 24 or 48 hrs. **d**) Representative traces from NTA illustrating the particle number/size in CD63-pHluorin-transfected and untransfected neurons. **e**) Bar graph showing no difference between both conditions ( $n = 3$ ,  $p = 0.0713$ ). Data are shown in mean  $\pm$  s.e.m. For comparison, a one-way ANOVA was used in **b**) and **c**) and a two-tailed unpaired t-test was used in **e**).  $**P < 0.01$ .

**Figure S4: Treatment with bFGF has no effect on neuronal cell death.** **a**) Bar graph illustrating that treatment with bFGF has no statistical significant effect on the release of lactate dehydrogenase (LDH) from cultured neurons when treated with bFGF for 24 hrs (left;  $n = 12$ ;  $p = 0.1553$ ) or 48 hrs (right;  $n = 12$ ;  $p = 0.0718$ ); positive control with 1% Triton X-100 for 15 min. **b,c**) Bar graph and photomicrograph illustrating a comparable average nuclear diameter in bFGF and VEH-treated cells (samples/condition  $n = 11804$  and  $8300$ ;  $p = 0.1021$ ) suggesting a comparable number of apoptotic nuclei subsequent to bFGF treatment. Data are shown as mean  $\pm$  s.e.m. For comparison, a two-tailed unpaired t-test was used.

**Figure S5 Treatment with bFGF has no effect on the number or size of late endosomes/MVBs.** a) Photomicrographs of cultured hippocampal neurons illustrating CD63-pHluorin-labeled endosomes in VEH- and bFGF-treated neurons (first and second row). To quantify their number and size, binary images (third row) were created from each group. Scale bar: 5  $\mu$ m. **b,c)** Treatment with bFGF has no effect on the size or number of CD63-pHluorin-labeled endosomes (particle number: VEH vs. bFGF cells/condition  $n = 98$  and  $102$ ;  $p = 0.9916$ ; particle area:  $p = 0.8690$ ). **d)** Representative electron microscope (EM) images from VEH- and bFGF-treated neurons stained with gold-conjugate labelled anti-GFP antibody. Scale bar: 1  $\mu$ m. **e,f)** Treatment with bFGF had no effect on the size or number of pHluorin-tagged MVBs (particle number: VEH vs. bFGF cells/condition  $n = 42$  and  $43$ ;  $p = 0.3415$ ; particle area:  $p = 0.0758$ ). Data are shown as mean  $\pm$  s.e.m. For comparison, a two-tailed unpaired t-test was used.

**Figure S6:** Correlation analysis of array replicates of VEH and bFGF treated exosomal pellets.

**Figure S7: Knockdown of *Vamp3* in bFGF-treated neurons.** a) Western blot illustrating a strong reduction of Vamp3 in response to transfection with *Vamp3* siRNAs and treatment with bFGF. **b)** Bar graph illustrating a reduced Vamp3 signal und Vamp3-siRNA transfected cells ( $n = 12$ /condition). Data are shown in mean  $\pm$  s.e.m. For comparison, a two-tailed unpaired t-test was used. \*\*\* $p < 0.001$ .

**Figure S8: Brain-derived neurotrophic factor (BDNF) and nerve growth factor (NGF) increase neuronal EV release.** a) Representative traces from NTA illustrating the particle number/size in cultured neurons treated with bFGF (50 ng/ml),

BDNF (25 ng/ml) or NGF (50 ng/ml) for 24 hrs. **b,c)** bFGF, BDNF and NGF increase the number of particles in the cell culture medium from cultured neurons without affecting particle size. ( $n = 8/\text{condition}$ ). Data are shown in mean  $\pm$  s.e.m. For comparison, a two-tailed, paired t-test was used.  $***p < 0.001$ .

**Figure S9: Treatment with bFGF differentially affects the abundance of EV-enriched proteins.** **a)** Representative Western blot pictures illustrating the protein abundance of Alix, CD81, CD9 and Flotilin-1 in EV-enriched medium pellets from cultured neurons. The respective treatment conditions are indicated above the Western blot. **b)** Bar graph illustrating the protein abundance of Alix, CD81, CD9 and Flotilin-1 in EV-enriched medium pellets from cultured neurons. Treatment of cultured neurons with bFGF has a differential effect on the abundance of the respective proteins in EV-enriched medium pellets. *Alix*: VEH + CON siRNA vs. bFGF + CON siRNA,  $n = 15$ ,  $p < 0,0001$ ; VEH + *Vamp3* siRNA vs. bFGF + *Vamp3* siRNA,  $n = 15$ ,  $****p < 0,0001$ . *CD81*: VEH + CON siRNA vs. bFGF + CON siRNA,  $n = 12$ ,  $***p = 0,001$ ; VEH + *Vamp3* siRNA vs. bFGF + *Vamp3* siRNA,  $n = 12$ ,  $**p = 0,002$ . *CD9*: VEH + CON siRNA vs. VEH + *Vamp3* siRNA,  $n = 6$ ,  $**p = 0,0032$ ; VEH + *Vamp3* siRNA vs. bFGF + *Vamp3* siRNA,  $n = 6$ ,  $****p < 0,0001$ . Data are shown in mean  $\pm$  s.e.m. For comparison, a one-way ANOVA with multiple comparisons was used.

**Figure S10: bFGF affects the abundance of EV-enriched proteins.** Bar graph illustrating the relative abundance of the ExoCarta (<http://www.exocarta.org>) top 100 EV-enriched proteins from VEH (blue) and bFGF-treated neurons (red) as measured by mass spectrometry. The data are extracted from the mass spectrometry measurement in table S1 with an equal total protein concentration in EV-enriched medium pellets from either treatment condition (VEH vs bFGF). Despite an equal



total protein concentration, the abundance of the listed proteins varies up to ~ 10 fold. Data are shown as mean value relative to the VEH condition (n = 6).

**Table S1: bFGF affects the abundance of EV-associated proteins.** Table indicating the top 1104 differentially abundant proteins in EV-enriched pellets in response to treatment with bFGF (50 ng ml<sup>-1</sup> for 24 hrs) including the gene names, log ratios and p-values.

**Table S2: Effect of bFGF on the abundance of the ExoCarta Top 100 exosomal marker proteins** ([http://exocarta.org/exosome\\_markers\\_new](http://exocarta.org/exosome_markers_new)).